Journal of Interdisciplinary Mathematics
ISSN: 0972-0502 (Print), ISSN: 2169-012X (Online)
Vol. 28 (2025), No. 7, pp. 2649–2676
DOI : 10.47974/JIM-2242

Evaluating the consequences of quarantine non-compliance on disease spread and control

Erlina Nita Sumadya [†]
Department of Mathematics
Faculty of Mathematics and Natural Sciences
Universitas Indonesia
Depok 16424
Indonesia

Bevina D. Handari *
Dipo Aldila [§]
Department of Mathematics
Faculty of Mathematics and Natural Sciences
Universitas Indonesia
Depok 16424
Indonesia

and

Innovative Mathematics and Predictive Analytics for Complex System and Technology Laboratory (IMPACT Lab)
Universitas Indonesia
Depok 16424
Indonesia

Bayu Prihandono [‡]
Department of Mathematics
Universitas Tanjungpura
Pontianak 78124
Indonesia

[†] *E-mail:* erlinanita@sci.ui.ac.id
* *E-mail:* bevina@sci.ui.ac.id (Corresponding Author)
[§] *E-mail:* aldiladipo@sci.ui.ac.id
[‡] *E-mail:* bayuprihandono@math.untan.ac.id

Abstract

We propose a mathematical model for disease transmission which incorporates the effect of non-compliance of quarantine intervention. This model uses the spread of infection in the form of a nonstandard population dependent ratio, where the total population involved in the infection process becomes dependent on time due to the effect of non-compliance people with the quarantine process. A detailed discussion was carried out on the model analysis regarding the effect of the reproduction number on the existence and stability of the equilibrium points. Model parameters were estimated using COVID-19 daily incidence data in Jakarta. Numerical experiments on the sensitivity analysis and autonomous simulations were given to give a better understanding on the impact of model parameters on disease control strategy. The experiment on the bifurcation diagram indicates the potential for recurring outbreaks in the population. As shown by the results of the sensitivity analysis, it was shown that probability of quarantine compliance has a negative relationship with the basic reproduction number. Numerical results also show that the transmission and recovery rate also have a significant influence on the spread and control of the disease.

Subject Classification: *00A69, 92B05.*

Keywords: *Quarantine, Non-compliance, Reproduction number, Sensitivity analysis, Bifurcation.*

1. Introduction

In the period after the COVID-19 pandemic from 2019 to 2022, valuable knowledge has been obtained regarding dangers associated with contagious illnesses. The collection of data becomes essential in order to ascertain the prospective consequences of diseases in the long term [1]. By utilising the existing data, we can predict the potential results if specific interventions are required to be executed in the population. There exist several interventions that have been extensively employed globally, contingent upon the specific nature of the disease. To mitigate infections resulting from direct touch with infected persons, the most efficient approach is to minimize contact. These objectives can be accomplished by enforcing social distancing measures, imposing lockdown, or even isolating infected persons [2]. Interventions of this nature have been used to diseases such as influenza, COVID-19, TB, and others.

In contrast to diseases transferred through direct contact, diseases carried by other vectors (such as mosquitoes, rats, etc.) necessitate a distinct approach to minimize transmission. Specifically, outdoor mosquito spraying, sometimes referred to as fumigation, is the most common approach for controlling dengue or malaria [3], which is spread by the bite of a female mosquito carrying the disease. Pathogens

transmitted through direct contact with contaminated surfaces, such as COVID-19, necessitate a distinct strategy for management. The most advised approach in such situations is to ensure cleanliness of surfaces and engage in hand hygiene after coming into contact with foreign surfaces [4].

Given the aforementioned explanation, it is evident that the most prevalent intervention for certain diseases is the isolation of individuals with the illness. Imposing quarantine on infected persons reduces the likelihood of susceptible others coming into contact with them [5]. The impact on economic activity is relatively less pronounced in comparison to measures such as lockdown. Quarantine facilitates the closer monitoring of infected persons to guarantee their adherence to the prescribed therapy by medical professionals. Therefore, it is reasonable to anticipate that their recovery will be substantially accelerated in comparison to not implementing quarantine measures. Nevertheless, the execution of quarantine encounters certain obstacles. One obstacle is that occasionally infected individuals fail to comply with their quarantine and may continue to participate in social activities.

Mathematical modelling has been extensively employed to explore disease transmission. For example, tons of papers were published during the pandemic of COVID-19 in order to give a better understanding on the potential of COVID-19 intervention ([6, 7, 8, 9, 10, 11, 12, 13, 14]). Other than COVID-19, mathematical modelling has been widely employed by researches to study other diseases, such as dengue ([15, 16, 17, 18, 19, 20]), malaria ([21, 22, 23, 24, 25]), tuberculosis ([26, 27, 28, 29, 30, 31, 32]), monkeypox ([33, 34, 35, 36]), HIV ([37, 38, 39]), and many more [40]. On the articles mentioned above, few articles discuss about the impact of quarantine on their model, especially when taking quarantine non-compliance into account.

In 2011, Safi and Gumel [41] introduced an interesting epidemiologic model with twelve compartments for human population by considering quarantine, isolation, and imperfect vaccine. Their model shows a possibility of backward bifurcation at basic reproduction number equal to one, implying a possibility of diseases existing despite when the reproduction number already less than one. On the other hand, Fredj and Cherif [42] employ a mathematical model to analyze the effect of quarantine in the spread of COVID-19. Parameter estimation using incidence data of COVID-19 from Tunisia were conducted to calibrate

their model with a real situation in the field. Another way to transmit COVID-19 through quarantine intervention was also discussed by Yu *et al.* in [43]. They include a mutant compartment in their model, and conclude that isolation and medical intervention success to suppress the spread of COVID-19. Further studies were also conducted by many authors discussing the effect of quarantine in different set of data, for an example by Gu *et al.* in [44] with Pakistan data, Alsheri *et al.* in [45] with Saudi Arabia data, Pandey *et al.* in [46] with Maharashtra data, and many more.

Babaei *et al.* in [47] developed a fractional order model for assessing how quarantine affects the spread of COVID-19. Pandey *et al.* in [46] also used fractional order approach to analyze their model with effect of quarantine in COVID-19 model. However, they also included the latent time in their model. A negative impact of quarantine for diabetics people was discussed by authors Kouidere *et al.* in [48]. An optimal control approach used to their model to analyze the cost-effectiveness of possible strategies in the field. A non-monotonic incidence rate and involvement of quarantine class in a epidemic model was discussed by Srivastava and Nilam in [49]. A combination between hospitalization and quarantine on monkeypox transmission were discussed by Musafir *et al.* in [50].

Among all the articles mentioned above, none addresses the impact of non-compliance with quarantine measures on disease spread. Therefore, the novelty of this research lies in the development of an epidemiological mathematical model that incorporates a nonstandard infection rate, where the population involved in the transmission process becomes time-dependent due to quarantine non-compliance. This means that the number of individuals contributing in transmitting the disease is not the entire population but depends on the number of people who adhere to or violate quarantine protocols. Those who follow quarantine correctly do not contribute to the spread of the disease. In this paper, a system of ordinary differential equations is used to build the model. The equilibrium points are examined in terms of existence and local stability, followed by the computation on the basic reproduction number and an investigation into its impact on the existence and stability of the equilibrium. Additionally, we conduct a global sensitivity analysis of the model. Finally, we perform numerical experiments to explore the impact of control parameters on disease dynamics.

The paper is structured as follows. In Section 1, we provide an introduction and review the state of the art. Section 2 is dedicated to the construction of the mathematical model and preliminary analysis of its biological properties. The analysis of equilibrium points and the basic reproduction number is presented in Section 3, while numerical experiments are discussed in Section 4. Finally, the conclusions drawn from both the analytical and numerical results are summarized in Section 5.

2. Model construction and preliminary analysis

2.1 *Model construction*

Assume that the human population is categorized into five compartments, namely the susceptible compartment S (a group where the individuals are vulnerable to the infection), infected compartment I (a group where all individuals are infected and able to spread the disease through a close contact), compliant quarantine compartment Q_1 (a group where all individuals are infected but unable to spread the disease due to a quarantine intervention), non-compliance quarantines compartment Q_2 (a group where all individuals are infected and still able to spread the disease due to non-compliance on a quarantine intervention) and recovered compartment R (a group where all individuals have recovered from the disease and has a permanent immunity to the disease). Several assumptions need to be stated before we developed the model.

(A1) The total number of individuals in the population follows: $N = S + I + Q_1 + Q_2 + R$.

(A2) Diseases only transmitted horizontally through close contact between S and I and Q_1.

(A3) Individuals in Q_1 can not transmit the disease, while Q_2 are able to transmit the disease.

(A4) Transmission rate of individuals in Q_2 are reduced by a factor $\xi \in [0,1]$.

(A5) Infection rate modelled as a population dependent function.

(A6) From the rate of quarantine intervention γ, only p proportion of them carry out quarantine obediently so that they cannot spread the infection to other people.

As shown in Figure 1, the diagram represents the model's transmission process.

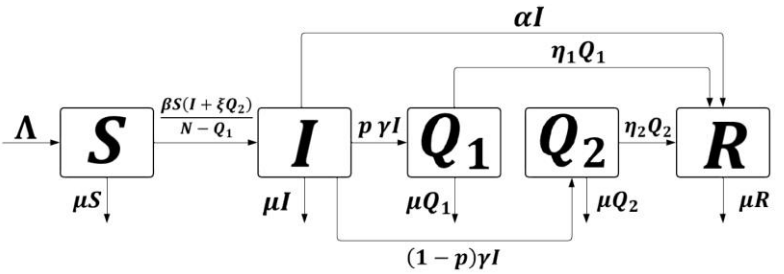

Figure 1
Diagram transmission of the model

The model derivation for each compartment is given as follows.

- **Susceptible compartment.** This group of individuals is increased due to new born with a rate of Λ, and decreases due to infection. Assuming a rate of successful infection is given by β, and assumption (A2), (A3), (A4), (A5), then we have the infection term is given by $\frac{\beta S(I+\xi Q_2)}{N-Q_1}$. Hence, the dynamic of S is given by $\frac{dS}{dt} = \Lambda - \frac{\beta S(I+\xi Q_2)}{N-Q_1} - \mu S$, where μ is the natural death rate.
- **Infected compartment.** The infected compartment increases due to a new infection given by $\frac{\beta S(I+\xi Q_2)}{N-Q_1}$, and decreases due to a quarantine intervention with a rate of γ, natural recovery rate α, and natural death rate μ. Hence, the rate of change of I is represented by $\frac{dI}{dt} = \frac{\beta S(I+\xi Q_2)}{N-Q_1} - (\gamma + \alpha + \mu)I$.
- **Compliant quarantine compartment.** Using assumption (A6), the increase in the Q_1 compartment is attributed to a quarantine intervention from I compartment with a proportion of p, and decreases due to recovery rate of η_1, and natural death rate μ. Hence, the model which represents the dynamic of Q_1 can be written as $\frac{dQ_1}{dt} = p\gamma I - (\eta_1 + \mu)Q_1$.
- **Non-compliant quarantine compartment.** With assumption (A6), the compartment Q_2 increases due to a quarantine intervention with a proportion of $1-p$, and decreases due to recovery rate η_2 and natural death rate μ. Hence, the dynamic of Q_2 is determined by $\frac{dQ_2}{dt} = (1-p)\gamma I - (\eta_2 + \mu)Q_2$.
- **Recovered compartment.** An increases in this compartment is due to recovery from I, Q_1, and Q_2 compartment with a rate of α, η_1,

and η_2, respectively. With a natural death rate μ, the dynamic of R is described by $\frac{dR}{dt} = \alpha I + \eta_1 Q_1 + \eta_2 Q_2 - \mu R$.

Based on above description, the mathematical model to describe the impact of non-compliance of quarantine is given as follows:

$$\frac{dS}{dt} = \Lambda - \frac{\beta S(I+\xi Q_2)}{N-Q_1} - \mu S, \frac{dI}{dt} = \frac{\beta S(I+\xi Q_2)}{N-Q_1} - (\gamma + \alpha + \mu)I,$$
$$\frac{dQ_1}{dt} = p\gamma I - (\eta_1 + \mu)Q_1, \frac{dQ_2}{dt} = (1-p)\gamma I - (\eta_2 + \mu)Q_2,$$
$$\frac{dR}{dt} = \alpha I + \eta_1 Q_1 + \eta_2 Q_2 - \mu R, \quad (1)$$

together with a non-negative initial condition, and satisfies $S(0) + I(0) + Q_1(0) + Q_2(0) + R(0) = \frac{\Lambda}{\mu}$.

2.2 *Parameterization of Model Parameters by Model Validation with Incidence Data*

In this chapter, parameter estimation is carried out for the model in equation (1) by finding the best parameters that can make the output of the model fit the field incident data. The field incident data used is active case incident data detected in Jakarta, which can be accessed in [51]. The goal of estimating these parameters can be described in the form of minimizing the following objective function:

$$\mathcal{J} = \sum_{i=0}^{T} (\text{Data} - (i) - (Q_1(i) + Q_2(i)))^2.$$

The function above aims to minimize the Euclidean distance from case incident data recorded in the field with the model output represented by the variables Q_1 and Q_2. To achieve this minimum value of $\mathcal{J}$, parameter values are needed that can make the model output as close as possible to the field data. The parameters to be estimated in this paper are: $\beta, \xi, \gamma, \alpha, \eta_1, \eta_2$, and p, as well as the initial values $S(0), I(0), Q_1(0), Q_2(0)$, and $R(0)$. The software used to estimate parameters is the MATLAB toolbox, in the form of *fmincon*. The corresponding results can be shown in Figure 2:

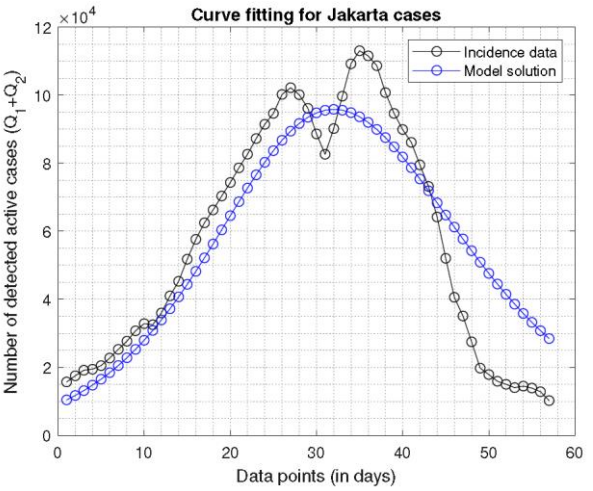

Figure 2
Parameter estimation results for Jakarta incidence data

The values of the parameters and the initial conditions are provided in Table 1:

Table 1
Parameter Values and Initial Conditions

Par	Interpretation	Unit	Value	Note
Λ	Birth rate	$\frac{\text{people}}{\text{time}}$	$\frac{10{,}560{,}000}{365\times73}$	estimated
β	Infection rate	$\frac{1}{\text{time}}$	0.364	fitted
ξ	Adjustment factor for non-compliance	-	0.482	fitted
μ	Natural death rate	$\frac{1}{\text{time}}$	$\frac{1}{365\times73}$	estimated
γ	Quarantine intervention rate	$\frac{1}{\text{time}}$	0.061	fitted
α	Natural recovery rate	$\frac{1}{\text{time}}$	0.198	fitted
η_1	Recovery rate for compliant quarantine	$\frac{1}{\text{time}}$	0.458	fitted
η_2	Recovery rate for non-compliant quarantine	$\frac{1}{\text{time}}$	0.290	fitted
p	Proportion of compliant individuals	-	0.389	fitted
$S(0)$	Initial condition of susceptible compartment	people	10,403,532	fitted
$I(0)$	Initial condition of infected compartment	people	88,390	fitted

$Q_1(0)$	Initial condition of compliant quarantine compartment	people	4,121	fitted
$Q_2(0)$	Initial condition of non-compliant quarantine compartment	people	6,305	fitted
$R(0)$	Initial condition of recovered compartment	people	10,361	fitted

2.3 *Non-dimensionalization of the model*

Assuming $x_1 = \frac{S}{N}, x_2 = \frac{I}{N}, x_3 = \frac{Q_1}{N}, x_4 = \frac{Q_2}{N}$, and $x_5 = \frac{R}{N}$, we get the non-dimensional version of system (1) which is given as follows:

$$\frac{dx_1}{dt} = \mu - \frac{\beta x_1(x_2+\xi x_4)}{1-x_3} - \mu x_1, \frac{dx_2}{dt} = \frac{\beta x_1(x_2+\xi x_4)}{1-x_3} - (\gamma + \alpha + \mu)x_2, \quad (2)$$

$$\frac{dx_3}{dt} = p\gamma x_2 - (\eta_1 + \mu)x_3, \frac{dx_4}{dt} = (1-p)\gamma x_2 - (\eta_2 + \mu)x_4,$$

with $x_5 = 1 - (x_1 + x_2 + x_3 + x_4)$.

2.4 *Preliminary analysis*

Theorem 1: *The simplified model in system (1) which is given by system (2) with initial conditions that are non-negative* $x_1(0) > 0, x_2 \geq 0, x_3 \geq 0, x_4 \geq 0, x_5 \geq 0$*, such that the model solutions, given non-negative initial data, remain stay non-negative for every* $t > 0$.

Proof: In the boundary plane of $\mathbb{R}^5_{\geq 0}$, we have:

$$\frac{dx_1}{dt}(x_1 = 0) = \mu > 0, \frac{dx_2}{dt}(x_2 = 0) = \frac{\beta x_1(x_2+\xi x_4)}{1-x_3} \geq 0, \frac{dx_3}{dt}(x_3 = 0) = p\gamma x_2,$$

$$\frac{dx_4}{dt}(x_4 = 0) = (1-p)\gamma x_2 \geq 0, \frac{dx_5}{dt}(x_5 = 0) = \alpha x_2 + \eta_1 x_3 + \eta_2 x_4 \geq 0.$$

It is clear that no direction along the boundary is negative, which means that all solutions will be repelled from the boundary toward the interior of $\mathbb{R}^5_{\geq 0}$. Consequently, for such nonnegative initial conditions, the solution will always be at least zero ($\mathbb{R}^5_{\geq 0}$). Furthermore, since the total population does not change over time, we have $\sum_{i=1}^5 x_i = 1$ at all times. Thus, we are only interested in the biologically feasible domain:

$$\Gamma = \left\{(x_1, x_2, x_3, x_4, x_5) \in \mathbf{R}^5_{\geq 0} : \sum_{i=1}^5 x_i = 1\right\}.$$

Since the total human population is constant, then we will only analyze the first four equations in (2), while x_5 can be calculated as $1 - x_1 - x_2 - x_3 - x_4$.

3. Model Analysis

In this part of the paper, we conduct a mathematical analysis to determine the existence and local stability criteria for all possible equilibria of the model in (2).

3.1 *Disease-free Equilibrium*

The first equilibrium of model (2) is the disease-free equilibrium point, which corresponds to the condition where the disease has been eradicated from the population. In this scenario, the system reaches the disease-free equilibrium when $I = Q_1 = Q_2 = 0$, indicating there are no quarantined or infected individuals. Therefore, the disease-free equilibrium point is given as follows:

$$X^{\dagger} = (x_1^{\dagger}, x_2^{\dagger}, x_3^{\dagger}, x_4^{\dagger}) = (1,0,0,0).$$

3.2 *Basic Reproduction Number*

In this chapter, we compute the basic reproduction number of our proposed model in (2). The basic reproduction number is extensively used by researchers to understand the qualitative dynamic of their models, particularly in determining the persistence criteria of diseases. We employ the next-generation matrix approach from [52] to compute the basic reproduction number for our model. For readers interested in seeing more examples of this method applied to other models, please refer to [53], [54], and [55].

To calculate $\mathcal{R}_0$, we consider all infected compartments in model (2), specifically I, Q_1, and Q_2. By performing a direct calculation, we derive the Jacobian matrix associated with the infected sub-compartments, evaluated at the disease-free equilibrium. This matrix, denoted by J, is given by:

$$J = \begin{bmatrix} \beta - (\gamma + \alpha + \mu) & 0 & \xi\beta \\ p\gamma & -(\eta_1 + \mu) & 0 \\ (1-p)\gamma & 0 & -(\eta_2 + \mu) \end{bmatrix}.$$

Write J as $F + V$, where F and V as the transmission matrix and the transition matrix consecutively.

$$F = \begin{bmatrix} \beta & 0 & \xi\beta \\ 0 & 0 & 0 \\ 0 & 0 & 0 \end{bmatrix}, V = \begin{bmatrix} -(\gamma + \alpha + \mu) & 0 & 0 \\ p\gamma & -(\eta_1 + \mu) & 0 \\ (1-p)\gamma & 0 & -(\eta_2 + \mu) \end{bmatrix}.$$

Since the second and the third row of F is all zero, then the next-generation matrix of system (2) is formulated by the following

formula $-E^T FV^{-1}E$, where $E^T = [1\ 0\ 0]$. Hence, the $\mathcal{R}_0$ is taken from spectral radius of the respected next-generation matrix and is represented by:

$$\mathcal{R}_0 = \frac{\beta(\gamma\xi(1-p)+\mu+\eta_2)}{(\eta_2+\mu)(\gamma+\alpha+\mu)}. \tag{3}$$

3.2 *Stability of The Disease-free Equilibrium*

Theorem 2: *The disease-free equilibrium of system (2), denoted by* $X^\dagger$*, is locally asymptotically stable if* $\mathcal{R}_0 < 1$*, and unstable if* $\mathcal{R}_0 > 1$.

Proof: By linearizing the model in (2) around the disease-free equlibruum, we have the J_{DFE}:

$$J_{\text{DFE}} = \begin{bmatrix} -\mu & -\beta & 0 & -\xi\beta \\ 0 & \beta-(\gamma+\alpha+\mu) & 0 & \xi\beta \\ 0 & p\gamma & -(\eta_1+\mu) & 0 \\ 0 & (1-p)\gamma & 0 & -(\eta_2+\mu) \end{bmatrix}.$$

The system is locally asymptotically stable if all the real parts of the eigenvalues of the corresponding matrix are negative. Two explicit eigenvalues of J_{DFE} are $-\mu$ and $-(\eta_1+\mu)$. The other two eigenvalues correspond to the roots of the following polynomial:

$$\lambda^2 + a_1\lambda + a_0 = 0,$$

where $a_1 = \alpha - \beta + \gamma + 2\mu + \eta_2$ and $a_0 = (\eta_2+\mu)(\gamma+\alpha+\mu)(1-\mathcal{R}_0)$. λ_3 and λ_4 will have a negative real part if a_0 and a_1 are positive. It can be seen that $a_0 > 0$ will be satisfied if $\mathcal{R}_0 < 1$. Furthermore, $a_1 > 0$ if $\frac{\beta}{\alpha+\gamma+2\mu+\eta_2,} < 1$. Since:

$$\frac{\beta}{\alpha+\gamma+2\mu+\eta_2} < \frac{\beta}{\alpha+\gamma+\mu+\eta_2} < \frac{\beta}{\alpha+\gamma+\mu} < \frac{\beta(\mu+\eta_2+\gamma\xi(1-p))}{(\alpha+\gamma+\mu)(\mu+\eta_2)} = \mathcal{R}_0,$$

then $a_1 > 0$ whenever $\mathcal{R}_0 < 1$. Hence the proof is complete.

3.4 *Analysis of the Existence of Endemic Equilibrium Point*

The second equilibrium of system (2) correspond to the non-trivial equilibrium, known as the endemic equilibrium ($X^\ddagger$). Setting the right-hand side of system (2) to zero and solving for x_1, x_2, x_3, and x_4 yields the following:

$$X^\ddagger = (x_1^\ddagger, x_2^\ddagger, x_3^\ddagger, x_4^\ddagger)$$

where $x_1^\ddagger = \frac{\gamma(\eta_1+\mu(1-p))+(\alpha+\mu)(\eta_1+\mu)}{\mathcal{R}_0((\eta_1+\mu)(\alpha+\mu)+\gamma\eta_1)+\gamma\mu(\mathcal{R}_0-p)}$, $x_2^\ddagger = \frac{\mu(\mu+\eta_1)(\mathcal{R}_0-1)}{\mathcal{R}_0((\eta_1+\mu)(\alpha+\mu)+\gamma\eta_1)+\gamma\mu(\mathcal{R}_0-p)}$, $x_3^\ddagger = \frac{p\mu\gamma(\mathcal{R}_0-1)}{\mathcal{R}_0((\eta_1+\mu)(\alpha+\mu)+\gamma\eta_1)+\gamma\mu(\mathcal{R}_0-p)}$,

and $x_4^{\ddagger} = \frac{\mu\gamma(\mu+\eta_1)(1-p)(\mathcal{R}_0-1)}{(\mathcal{R}_0((\eta_1+\mu)(\alpha+\mu)+\gamma\eta_1)+\gamma\mu(\mathcal{R}_0-p))(\eta_2+\mu)}$.

From the expression of $x_i^{\ddagger}$ for $i = 1,2,3,4$ above, this theorem about the existence criteria of the endemic equilibrium point is defined as follows:

Theorem 3: *The endemic equilibrium of model in system (2) always exists and unique if* $\mathcal{R}_0 > 1$*, and no endemic equilibrium otherwise.*

3.5 *Stability of the Endemic Equilibrium*

This section analyzes the stability of the endemic equilibrium point in system (2). The difficulty of linearizing the model to the endemic equilibrium prompted us to employ the Castillo-Song Theorem [56] to assess the local stability of the endemic point. The system (2) includes the bifurcation parameter β. The Castillo-Song Theorem is applied when $\mathcal{R}_0 = 1$. Substituting $\mathcal{R}_0 = 1$ into equation (3), we obtain the equation for β that satisfies $\mathcal{R}_0 = 1$ as $\beta^* = \frac{\alpha\mu+\alpha\eta_2+\gamma\mu+\gamma\eta_2+\mu^2+\mu\eta_2}{\gamma p\xi(1-p)+\mu+\eta_2}$. By linearizing the system (2), the jacobian matrix evaluated at $\beta = \beta^*$ and $x^{\dagger}$ gives the following eigenvalues: $\lambda_1 = -\mu$, $\lambda_2 = -(\mu+\eta_1)$, $\lambda_3 = -\frac{\xi(1-p)\gamma^2+2(1-p)\left(\mu+\frac{1}{2}\alpha+\frac{1}{2}\eta_2\right)\xi\gamma+(\eta_2+\mu)^2}{\xi(1-p)\gamma+\mu+\eta_2}$, and $\lambda_4 = 0$.

Note that the matrix J^* possesses a simple eigenvalue at zero, and the rest are negative. Based on this, the conditions of the Castillo-Song theorem are satisfied. Next, the stability analysis of the endemic equilibrium point is investigated using the Castillo-Song theorem. The first step is to find the right and left eigenvectors associated with eigenvalue 0. The right eigenvectors of J^* correspond to $\lambda = 0$ are:

$$w_1 = -\frac{(\eta_1+\mu)(\gamma+\alpha+\mu)w_3}{p\mu\gamma}, w_2 = \frac{(\eta_1+\mu)c}{\gamma p}, w_3 = w_3, w_4 = \frac{(1-p)(\eta_1+\mu)c}{(\eta_2+\mu)p}.$$

On the other hand, the left eigenvectors associated with the eigenvalue 0 are:

$$v_1 = 0, v_2 = \frac{(\gamma\xi(1-p)+\mu+\eta_2)v_4}{(\gamma+\alpha+\mu)\xi}, v_3 = 0, v_4 = v_4.$$

Afterward, $\mathcal{A}$ and $\mathcal{B}$ will be computed using the following formula:

$$\mathcal{A} = \sum_{k=1}^{n}\sum_{i=1}^{n}\sum_{j=1}^{n} v_k w_i w_j \frac{\partial^2 f_k}{\partial x_i \partial x_j}(0,0), \mathcal{B} = \sum_{k=1}^{n}\sum_{i=1}^{n} v_k w_i \frac{\partial^2 f_k}{\partial x_i \partial \phi}(0,0).$$

From direct calculation, $\mathcal{A}$ and $\mathcal{B}$ is given by:

$$\mathcal{A} = -\frac{2\beta\mu(x_1)(x_2+x_3)}{x_4},$$
$$\mathcal{B} = \frac{\mu}{\gamma+\alpha+\mu} + \frac{\xi(1-p)\gamma\mu}{\eta_2(\gamma+\alpha+\mu)+\mu(\gamma+\alpha+\mu)},$$

with $x_1 = (1-p)\mu + \eta_1)\gamma + (\eta_1+\mu)(\alpha+\mu)$, $x_2 = \eta_2(\gamma+\alpha+\mu) + \mu(\gamma+\alpha+\mu)$, $x_3 = (1-p)\xi\mu + (1-p)\xi\alpha)\gamma$, and $x_4 = \eta_2(\gamma+\alpha+\mu) + \mu((\gamma+\alpha+\mu)^2(\eta_2(\gamma+\alpha+\mu) + \mu(\gamma+\alpha+\mu))(\eta_1+\mu)$. Based on this, we have obtained $\mathcal{A} < 0$ and $\mathcal{B} > 0$. Based on the Castillo-Song Theorem, the endemic equilibrium point does not exist when $\mathcal{R}_0 < 1$, and simultaneously, the disease-free equilibrium point is stable. When $\mathcal{R}_0 = 1$, changes in the existence and stability characteristics of both equilibrium points occur. Furthermore, when $\mathcal{R}_0 > 1$ the existence and stability characteristics of both equilibrium point change. Therefore, the conclusion is drawn that the existence and stability of an endemic equilibrium point is only guaranteed when $\mathcal{R}_0 > 1$, but close to one. Based on the calculation above, we derived the following theorem.

Theorem 4: The Endemic equilibrium $X^{\ddagger}$ of system (2) is locally stable when $\mathcal{R}_0 > 1$, but close to one.

4. Numerical Simulation and Discussion

This chapter presents a detailed discussion of analytical studies on the presence of endemic points and the role of the basic reproduction number. All parameters used were obtained from the parameter estimation results in chapter 2.2.

4.1 *Global sensitivity analysis*

In this section, we analyze the sensitivity of each parameter to the reproduction number using global sensitivity analysis with the Partial Rank Correlation Coefficient (PRCC) method and Latin Hypercube Sampling (LHS). The parameter values given in Table 1 are used as the base values, while the sampling intervals range from 50% to 150% of the estimated parameter values. We conduct the PRCC sensitivity analysis only for the controllable parameters in the $\mathcal{R}_0$ formula, namely $\beta, \xi, \gamma, \alpha, \eta_2$, and p. The results are shown in Figure 3.

All p-values are less than 0.05, indicating that all parameters significantly impact the value of $\mathcal{R}_0$. The infection parameter β and the adjustment factor for the infection rate of non-compliant individuals, ξ, have positive PRCC values, indicating that larger values of these

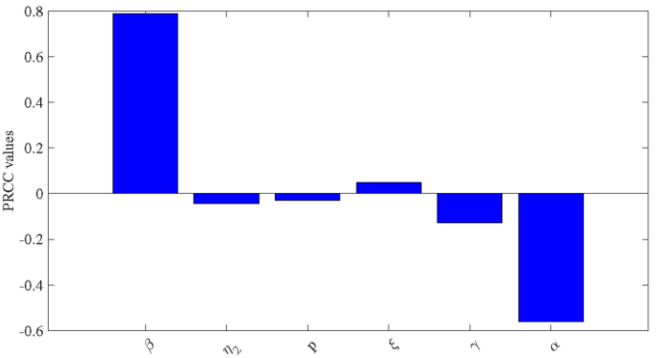

Figure 3
PRCC values on $\mathcal{R}_0$

parameters increase $\mathcal{R}_0$. On the other hand, the PRCC values for the recovery rate of compliant quarantined individuals (η_2), the proportion of compliant individuals (p), the intervention rate for quarantine (γ), and the natural recovery rate (α) are all negative. This means that increasing these parameters will make $\mathcal{R}_0$ smaller. Furthermore, it is evident that β has the most significant PRCC value, followed by α, γ, η_2, ξ, and p, respectively. This indicates that controlling the value of β will reduce $\mathcal{R}_0$ more significantly compared to the other parameters. Various strategies can be employed to control β, such as implementing social distancing, promoting self-protection against infection or direct contact, and so on. On the other hand, increasing α, which represents the natural recovery rate without quarantine intervention, can also greatly reduce $\mathcal{R}_0$. Interestingly, the proportion of individuals who comply with quarantine appears to be less significant than other parameters. One possible explanation is that the estimated values of the natural recovery rate α is much higher than the quarantine rate γ (please see Table 1), meaning that individuals are more likely to recover before requiring quarantine.

Effect of p

Then, this section discusses the effect of the person's probability of quarantine p on changes in the value of $\mathcal{R}_0$ and the equilibrium point values of all variables. The outcomes are illustrated in figure 4. In figure 4(a), it can be observed that as the value of p increased, the value of $\mathcal{R}_0$ decreased. This is in accordance with the results of global sensitivity

analysis where the PRCC value of p is negative. Based on the PRCC value analysis, the meaning is that the higher the chance of people carrying out quarantine, the population will free from disease. From the calculation results, it is known that $\mathcal{R}_0 = 1$ when $p = 0.835$.

In Figure 4(d), the ratio of the population of people who comply with quarantine (x_3) to the probability variable of quarantine people (p) has a non-trivial relationship. The obtained value of $p^* = 0.835$. When $p < 0.835$, it could mean that compliance quarantine efforts have not been maximized resulting in the number of x_3 continuing to increase. In contrast, if $p > p^*$ can mean that the quarantine effort has gone well, resulting in a significant decrease in the number of infected people (I), automatically causing the supply to x_3 and x_4 to decrease.

Therefore, if $p > 0.835$, then endemic points will not appear, and if $p = 0.835$, then endemic points will appear. This can be seen in the figures 4(b)-4(c) and 4(e)-4(f), when $p = 0.835$, the population x_1 increases, while the population x_2, x_4, and x_5 continue to decrease. However, when $p = 0.835$, then the total population is 1, all of which are x_1, while the other populations have a value of 0.

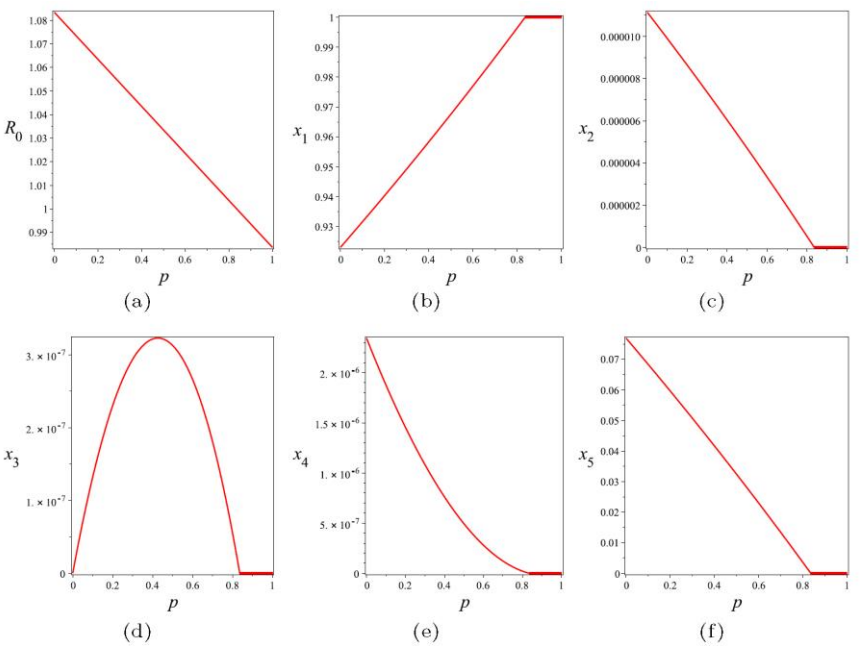

Figure 4

Effect of p on the size of $\mathcal{R}_0$ and all equilibrium points

4.2 *Two-parameter sensitivity analysis*

This section analyzes about the impact of two parameters on the sensitivity of the contour of $\mathcal{R}_0$, which is illustrated in Figure 5. The parameters used are the same as the previous parameters, except for β, which is reduced by 30%, while β and γ are treated as free parameters. Substituting these parameter values into $\mathcal{R}_0$ and plotting it as a contour plot yields the contour shown in Figure 5(a). It is evident that increasing β raises $\mathcal{R}_0$, while increasing γ reduces $\mathcal{R}_0$.

Reducing β as the rate of disease spread can be done by creating Large-Scale Social Restriction policies. With this policy, there will be a decrease in interaction between communities so that the rate of spread will also decrease. Meanwhile, increasing γ as a quarantine rate can be done by creating a policy through an Antigen Swab Test or PCR Test, namely that people who get positive test results for Covid disease are required to quarantine at home or hospital. This is supported by the policy of prohibiting people who test positive from using public facilities and transportation.

To show the impact of the combination between β and γ on the dynamic of model in system (2), we choose two sample point in Figure 5(a) which represent $\mathcal{R}_0 < 1$ and $\mathcal{R}_0 > 1$, and solve system (2) numerically using Runge-Kutta method which available in Matlab.

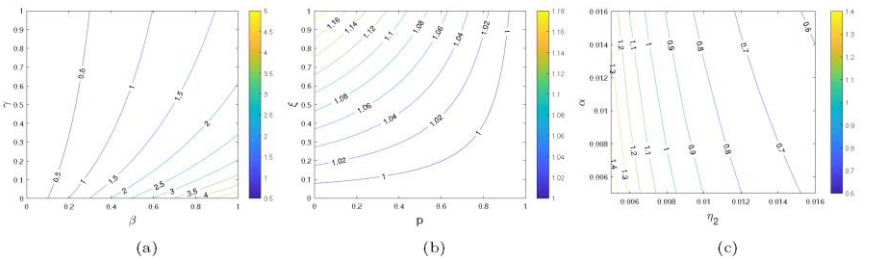

Figure 5
Sensitivity of $\mathcal{R}_0$ respect to Parameters

And then, it's analization the impact of two parameters p and ξ on the sensitivity of the contour of $\mathcal{R}_0$. Substituting these parameter values into $\mathcal{R}_0$ and plotting it as a contour plot yields the contour shown in Figure 5(b). It is evident that increasing p reduces $\mathcal{R}_0$, while increasing ξ raises $\mathcal{R}_0$.

Increasing p can be achieved through extensive socialization about the importance of complying with quarantine measures. Conversely,

reducing ξ can be accomplished by intensifying media campaigns about social distancing or by restricting access to public facilities for infected individuals. To analyze the impact of the combination between p and ξ on the dynamic of model in system (2), we choose two sample points in Figure 5(b) which represent $\mathcal{R}_0 < 1$ and $\mathcal{R}_0 > 1$, and solve system (2) numerically using Runge-Kutta method which available in Matlab.

Next, the analysis of the impact of two parameters α and η_2 on the sensitivity of the contour of $\mathcal{R}_0$. Substituting these parameter values into $\mathcal{R}_0$ and plotting it as a contour plot yields the contour shown in Figure 5(c). It is evident that increasing α and η_2 reduces $\mathcal{R}_0$.

Increasing α and η_2 can be achieved by improving health services, such as the availability of medicines, adequate inpatient places, and enough doctors in each health facility. To show the impact of the combination between α and η_2 on the dynamic of model in system (2), we choose two sample points in Figure 5(c) which represent $\mathcal{R}_0 < 1$ and $\mathcal{R}_0 > 1$, and solve system (2) numerically using Runge-Kutta method which available in Matlab.

4.3 *Bifurcation diagram*

From our previous analysis, the proposed model has the following properties: the disease-free equilibrium is stable only if $\mathcal{R}_0 < 1$, and becomes unstable when $\mathcal{R}_0 > 1$. Therefore, $\mathcal{R}_0 = 1$ serves as the bifurcation point. Additionally, the model has a unique endemic equilibrium when $\mathcal{R}_0 > 1$. From our bifurcation analysis, we reveal that the model consistently exhibits a forward bifurcation at $\mathcal{R}_0 = 1$.

This section focuses on conducting a numerical experiment to examine the bifurcation diagram of our model, using b as the bifurcation parameter under two different scenarios: $\eta_1 = 0.001$ and $\eta_1 = 0.9$. All other parameter values remain the same as those estimated in the previous section. For both scenarios, the forward bifurcation diagrams are shown in Figures 6 and 7, corresponding to $\eta_1 = 0.9$ and $\eta_1 = 0.001$, respectively. For both scenario, we identify $b = 0.25225$ as the branching point (BP). In the scenario with $\eta_1 = 0.9$, we observe that for any value of $b < BP$, the disease-free equilibrium is stable, but it loses stability as b crosses the branching point. Simultaneously, an increase in b leads to the emergence of a stable endemic equilibrium, indicated by the solid blue line.

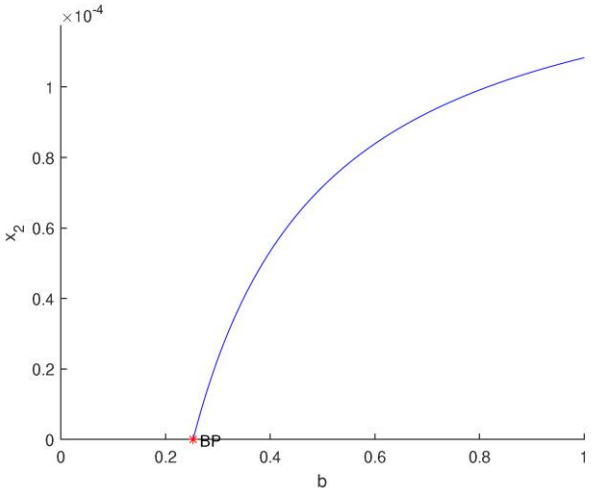

Figure 6

Transcritical bifurcation diagram of model (2) where $\eta_1 = 0.9$.

In the second scenario, we change the value of η_1 to 0.001, and the results are shown in Figure 7. The branching point at $\mathcal{R}_0 = 1$ remains the same as in the previous simulation, occurring at $b = 0.25225$. As b begins to move away from the branching point, a stable endemic equilibrium begins to emerge, eventually reaching its first Hopf point H_1 at $b = 0.27988$. This indicates a change occuring in the stability of the endemic equilibrium point. The endemic equilibrium becomes unstable and transitions into a stable periodic solution for $b > 0.27988$ until it reaches the second Hopf point H_2 at $b = 0.35797$. Beyond H_2, the endemic equilibrium regains its asymptotic stability and remains stable for any $b > 0.35797$. Some families of stable limit cycles for $b \in (0.27988, 0.35797)$ are illustrated in Figures 7(a)-7(b).

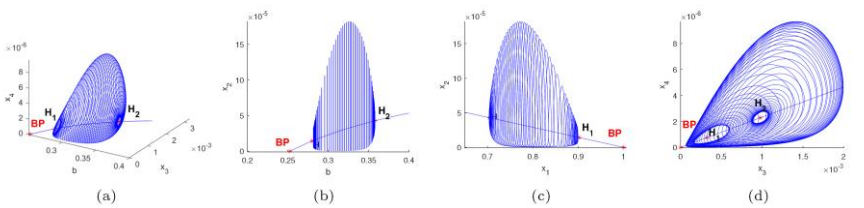

Figure 7

Transcritical bifurcation diagram of model (2) where $\eta_1 = 0.001$.

4.4 *Autonomous Simulation*

4.4.1 Improve Quarantine Rate

The following is an autonomous simulation of the difference in quarantine rate values (γ) in the Infected Compartment (I), the Compliant Quarantine Compartment (Q_1), and the Non-Compliant Quarantine Compartment (Q_2), as displayed in Figure 8. In these three compartments, there are two scenarios that occur when conditions are endemic in the blue graph ($\mathcal{R}_0 > 1$) and conditions free from disease in the red graph ($\mathcal{R}_0 < 1$).

Note that when $\gamma = 0.4$, the value $\mathcal{R}_0 = 0.94$, indicates the disease is no longer spreading. This will of course result in the condition ending in a disease-free condition, namely all compartments are in the Susceptible Compartment (S) and the other compartments have a value of zero. Meanwhile, when $\gamma = 0.2$, where $\mathcal{R}_0 = 1.20$, it can be seen that the graph has a much higher endemic peak than the graph when $\gamma = 0.4$. This means that under these conditions, the disease is still significantly contagious so that it has a peak point in 8(a) of almost 200,000 people. This endemic condition will end in a stable state in:

$$E^* = (S^*, I^*, Q_1^*, Q_2^*, R^*) = (8.73 \times 10^6, 172{,}29{,}73{,}1.86 \times 10^6)$$

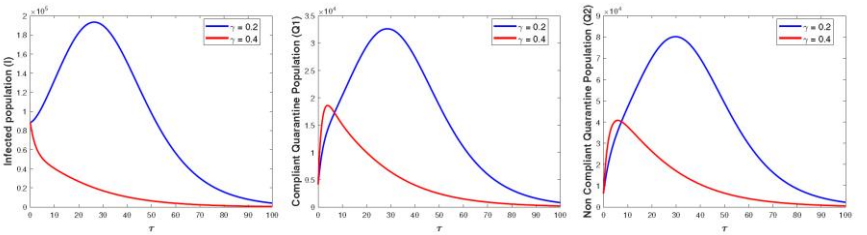

Figure 8
Simulation about Intervention to Improve Health Services when $\beta = 0.4$

4.4.2 Intervention Compliant of Quarantine

This subsection discusses the autonomous simulation of the difference in proportion of compliant individuals (p) as shown in Figure 9. Note that when $p = 0.8$, the value $\mathcal{R}_0 = 0.99$, indicates the disease is no longer spreading. This will of course result in the condition ending in a disease-free condition, namely all compartments are in the Susceptible Compartment (S) and the other compartments have a value of zero.

Meanwhile, when $p = 0.3$, where $\mathcal{R}_0 = 1.01$, it can be seen that the graph has a much higher endemic than the graph when $p = 0.8$ in 9(a). This endemic condition will end in a stable state in:

$$E^* = (S^*, I^*, Q_1^*, Q_2^*, R^*) = (1.04 \times 10^7, 19,1,3,1.31 \times 10^5).$$

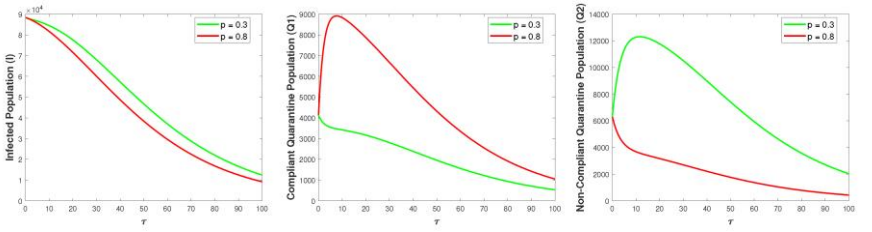

Figure 9

Simulation Intervention Compliant with Quarantine when $\xi = 0.2$.

Based on autonomous simulations from sub-chapters 4.4.1 to 4.4.2, it can be concluded that a single intervention can be carried out to reduce the level of disease spread in the population, even though other interventions have not changed (the intervention has not decreased or increased). For example, in sub-chapter 4.4.1, if the funds owned by the government are sufficient, while the community cannot comply with social power policies due to economic demands, then the government can reduce the spread of disease by improving health facilities (α). Apart from that, in sub-chapter 4.4.2, if the public's awareness of wearing masks as an effort to reduce the rate of spread of disease (ξ) is still very low, the government policy implemented is to make a firm appeal to the public to do so (p increases).

5. Conclusion

A mathematical model with the intervention of quarantine is discussed in this article. The reality that people do not always obey quarantine rules is incorporated into the model, allowing individuals who are non-compliant with quarantine to spread the disease to susceptible individuals. The key innovation of the proposed model is in the infection function, which has a non-standard dependency ratio where the total population involved in the infection process depends on the number of people who are non-compliant with the quarantine measures.

A detailed model analysis is conducted regarding the existence and local stability of equilibrium points, and how they are connected to the basic reproduction number. We found that the disease-free equilibrium is locally stable if $\mathcal{R}_0 < 1$ and unstable if $\mathcal{R}_0 > 1$. Furthermore, the model exhibits a unique endemic equilibrium, which exists and is stable only if $\mathcal{R}_0 > 1$.

Real-life testing of our model involved estimating its parameter using COVID-19 incident data in 2020 between March 5 and June 5 in Jakarta, Indonesia. To achieve a disease-free condition, parameter sensitivity analysis was carried out to determine an effective control strategy. With the estimated model parameters, we conducted a global sensitivity analysis. We found that the infection and recovery rates have the most significant impact on determining the magnitude of the basic reproduction number. Surprisingly, although the quarantine rate has a substantial impact on the basic reproduction number, the proportion of people complying with quarantine does not significantly affect its magnitude. However, we demonstrate that increasing both the quarantine rate and the proportion of people complying with quarantine can reduce the basic reproduction number. Another non-trivial result is that the recovery rate of compliant individuals does not explicitly included in the basic reproduction number. This is likely because individuals who comply with quarantine are not involved in the infection process. Although the recovery rate of compliant quarantined individuals has no impact on the size of the basic reproduction number, our numerical experiments show that this parameter still influences the size of each compartment in the endemic equilibrium. Furthermore, our numerical experiment on the bifurcation diagram regarding the impact of η_1 reveals an interesting phenomenon. We observe that when η_1 is significantly smaller than η_2, a stable periodic solution may emerge at $\mathcal{R}_0 > 1$. This phenomenon suggests a more challenging scenario for disease eradication, as the presence of a stable periodic solution indicates the potential for recurring outbreaks in the population.

Although our model incorporates the role of non-compliant individuals in quarantine, we have not yet considered how the quarantine rate and the proportion of people complying with quarantine might vary depending on the endemic level of the disease. In real-life situations, these factors could change dynamically: as the disease becomes more widespread, more people may voluntarily enter

quarantine, and compliance with quarantine protocols may increase. Therefore, future work should address this by modeling the quarantine rate and compliance proportion as functions of the disease's endemic level. A promising direction to explore this dynamic behavior is by extending our model into an optimal control problem, where the objective would be to determine the best strategies for adjusting quarantine measures based on the current state of the epidemic. This could provide insights into the most effective ways to control disease spread while considering varying compliance rates during different stages of an outbreak.

Acknowledgements

The second author is financially supported by Faculty of Mathematics and Natural Sciences, Universitas Indonesia (FMIPA-UI) with matching fund research grant scheme between FMIPA UI and FMIPA UNTAN, 2024 (ID Number: PKS-001/UN2.F3.D/PPM.00.02/2024). The third author is finacially supported by the Ministry of Research, Technology and Higher Education Indonesia (ID number : NKB-894/UN2.RST/HKP.05.00/2024).

References

[1] M. Cascella, M. Rajnik, S. C. Dulebohn, and R. Di Napoli, *Features, Evaluation, and Treatment of Coronavirus (COVID-19)*. StatPearls Publishing LLC (2023), available via: https://www.ncbi.nlm.nih.gov/books/NBK554776/.

[2] C. Murphy, W. W. Lim, C. Mills, J. Y. Wong, D. Chen, Y. Xie, M. Li, S. Gould, H. Xin, J. K. Cheung, S. Bhatt, B. J. Cowling, and C. A. Donnelly, "Effectiveness of social distancing measures and lockdowns for reducing transmission of covid-19 in non-healthcare, community based settings," *Philosophical Transactions of the Royal Society B: Biological Sciences*, vol. 378, no. 1877, p. 20210377 (2023).

[3] H. Onen, M. M. Luzala, S. Kigozi, R. M. Sikumbili, C.-J. K. Muanga, E. N. Zola, S. N. Wendji, A. B. Buya, A. Balciunaitiene, J. Viškelis, M. A. Kaddumukasa, and P. B. Memvanga, "Mosquito-borne diseases and their control strategies: An overview focused on green synthesized plant-based metallic nanoparticles," *Molecules*, vol. 28, no. 16, p. 5951 (2023).

[4] M. N. Khatib, A. Sinha, G. Mishra, S. Z. Quazi, S. Gaidhane, D. Saxena, A. M. Gaidhane, P. Bhardwaj, S. Sawleshwarkar, and Q. S. Zahiruddin, "Wash to control covid-19: A rapid review," *Clinical Epidemiology and Global Health*, vol. 16, p. 101101 (2022).

[5] B. Nussbaumer-Streit, V. Mayr, A. I. Dobrescu, A. Chapman, E. Persad, I. Klerings, G. Wagner, U. Siebert, C. Christof, C. Zachariah, and G. Gartlehner, "Quarantine alone or in combination with other public health measures to control covid-19: a rapid review," *The Cochrane Collaboration* (2020).

[6] M. A. Rois, Fatmawati, C. Alfiniyah, S. Martini, D. Aldila, and F. Nyabadza, "Modeling and optimal control of covid-19 with comorbidity and three-dose vaccination in indonesia," *Journal of Biosafety and Biosecurity*, vol. 6, no. 1, pp. 36–43 (2024).

[7] C. K. Mahadhika and D. Aldila, "A deterministic transmission model for analytics-driven optimization of covid-19 post-pandemic vaccination and quarantine strategies," *Mathematical Biosciences and Engineering*, vol. 21 (2024).

[8] F. Novkaniza, M. M. M. Malik, I. M. Sulaiman, and D. Aldila, "Modified spectral conjugate gradient iterative scheme for unconstrained optimization problems with application on covid-19 mode," *Frontiers in Applied Mathematics and Statistics*, vol. 8 (2022).

[9] D. Aldila, M. Shahzad, S. H. Khoshnaw, M. Ali, F. Sultan, A. Islamilova, Y. R. Anwar, and B. M. Samiadji, "Optimal control problem arising from covid-19 transmission model with rapid-test," *Results in Physics*, vol. 33, p. 105225 (2022).

[10] R. Prabakaran, S. Jemimah, P. Rawat, D. Sharma, and M. M. Gromiha, "A novel hybrid seiqr model incorporating the effect of quarantine and lockdown regulations for covid-19," *Scientific Reports* (2021).

[11] A. Mustapha, S. Musa, M. Abdullahia, and A. Husseini, "Mathematical modelling of covid-19 with vaccination, quarantine and non-pharmaceutical interventions," *International Journal of Development Mathematics*, vol. 1, no. 1, pp. 153–171 (2024).

[12] V. Bhatnagar, R. C. Poonia, P. Nagar, S. Kumar, V. Singh, L. Raja, and P. Dass, "Descriptive analysis of covid-19 patients in the context of india," *Journal of Interdisciplinary Mathematics*, vol. 24, no. 3, pp. 489–504 (2021).

[13] L. Ismail, H. Djellout, and C. Chauvière, "Global sensitivity analysis in the sihr epidemiological model with application to covid-19," *Journal of Statistics and Management Systems*, vol. 27, no. 7, pp. 1277–1299 (2024).

[14] V. Singh, R. C. Poonia, S. Kumar, P. Dass, P. Agarwal, V. Bhatnagar, and L. Raja, "Prediction of covid-19 corona virus pandemic based on time series data using support vector machine," *Journal of Discrete Mathematical Sciences and Cryptography*, vol. 23, no. 8, pp. 1583–1597 (2020).

[15] E. L. Megawati and D. Aldila, "A stability and optimal control analysis on a dengue transmission model with mosquito repellent," *Communications in Mathematical Biology and Neuroscience*, vol. 2023 (2023).

[16] D. Aldila, J. P. Ch´avez, C. W. Chukwu, A. Y. Fathiyah, J. W. Puspita, K. A. D. Setio, A. Fuady, and P. Z. Kamalia, "Unraveling dengue dynamics with data calibration from palu and jakarta: Optimizing active surveillance and fogging interventions," *Chaos, Solitons & Fractals*, vol. 189, p. 115729 (2024). [Online]. Available: https://www.sciencedirect.com/science/article/pii/S0960077924012815

[17] D. Aldila, C. A. Puspadani, and R. Rusin, "Mathematical analysis of the impact of community ignorance on the population dynamics of dengue," *Frontiers in Applied Mathematics and Statistics*, vol. 9 (2023).

[18] K. P. Wijaya, D. Aldila, K. K. W. H. Erandi, M. Fakhruddin, M. Amadi, and N. Ganegoda, "Learning from panel data of dengue incidence and meteorological factors in jakarta, indonesia," *Mathematical Biosciences*, vol. 35, pp. 437–456 (2021).

[19] A. Din, T. Khan, Y. Li, H. Tahir, A. Khan, and W. A. Kha, "Mathematical analysis of dengue stochastic epidemic model," *Results in Physics* (2021).

[20] S. A. Carvalho, S. O. da Silva, and I. da Cunha Charret, "Mathematical modeling of dengue epidemic: Control methods and vaccination strategies," *Theory in Biosciences*, vol. 138, pp. 223–239 (2019).

[21] I. H. Febiriana, D. Aldila, B. D. Handari, P. B. S. Asih, and M. H. N. Aziz, "Exploring the interplay between social awareness and the use of bed nets in a malaria control program," *Journal of Biosafety and Biosecurity*, vol. 6, pp. 196–210 (2024).

[22] I. H. Febiriana, A. H. Hassan, and D. Aldila, "Enhancing malaria control strategy: Optimal control and cost-effectiveness analysis on the

impact of vector bias on the efficacy of mosquito repellent and hospitalization," *Journal of Applied Mathematics* (2024).

[23] B. D. Handari, D. Aldila, E. Tamalia, S. H. A. Khoshnaw, and M. Shahzad, "Assessing the impact of medical treatment and fumigation on the superinfection of malaria: A study of sensitivity analysis," *Communications in Biomathematical Sciences*, vol. 6, no. 1, pp. 51–73 (2023).

[24] S. Tchoumi, H. Rwezaura, and J. Tchuenche, "A mathematical model with numerical simulations for malaria transmission dynamics with differential susceptibility and partial immunity," *Healthcare Analytics,* vol. 3 (2023).

[25] A. T. Haringo, L. L. Obsu, and F. K. Bushu, "A mathematical model of malaria transmission with media-awareness and treatment interventions," *Applied Mathematics and Computing*, vol. 70, pp. 4715–4753 (2024).

[26] D. Aldila, D. A. Ramadhan, C. W. Chukwu, B. D. Handari, M. Shahzad, and P. Z. Kamalia, "On the role of early case detection and treatment failure in controlling tuberculosis transmission: A mathematical modeling study," *Communications in Biomathematical Sciences*, vol. 7, no. 1, pp. 61–86 (2024).

[27] E. D. Ginting, D. Aldila, and I. H. Febiriana, "A deterministic compartment model for analyzing tuberculosis dynamics considering vaccination and reinfection," *Healthcare Analytics*, vol. 5 (2024).

[28] D. Aldila, B. L. Fardian, C. W. Chukwu, M. H. N. Aziz, and P. Z. Kamalia, "Improving tuberculosis control: Assessing the value of medical masks and case detection a multi-country study with costeffectiveness analysis," *Royal Society Open Science*, vol. 11 (2024).

[29] K. Oshinubi, O. J. Peter, E. Addai, E. Mwizerwa, O. Babasola, I. V. Nwabufo, I. Sane, U. M. Adam, A. Adeniji, and J. O. Agbaje, "Mathematical modelling of tuberculosis outbreak in an east african country incorporating vaccination and treatment," *Computation*, vol. 11, no. 7, p. 13 (2023).

[30] A. Malek and A. Hoque, "Mathematical model of tuberculosis with seasonality, detection, and treatment," *Informatics in Medicine Unlocked,* vol. 49 (2024).

[31] H. A. Fatahillah and D. Aldila, "Forward and backward bifurcation analysis from an imperfect vaccine efficacy model with saturated

treatment and saturated infection," *Jambura Journal of Biomath*, vol. 5, no. 2, pp. 132–143 (2024).

[32] O. J. Peter, D. Aldila, T. A. Ayoola, G. B. Balogun, and F. A. Oguntolu, "Modeling tuberculosis dynamics with vaccination and treatment strategies," *Scientific African*, vol. 28, p. e02647 (2025). [Online]. Available: https://www.sciencedirect.com/science/article/pii/S2468227625001176

[33] A. H. Hassan, D. Aldila, and M. H. N. Aziz, "Optimal control and stability analysis of monkeypox transmission dynamics with the impact of contaminated surfaces," *Applied Mathematics and Statistics*, vol. 10 (2024).

[34] B. Liu, S. Farid, S. Ullah, M. Altanji, R. Nawaz, and S. W. Teklu, "Mathematical assessment of monkeypox disease with the impact of vaccination using a fractional epidemiological modeling approach," *Scientific Reports* (2023).

[35] O. J. Peter, S. Kumar, N. Kumari, F. A. Oguntolu, K. Oshinubi, and R. Musa, "Transmission dynamics of monkeypox virus: a mathematical modelling approach," *Modeling Earth Systems and Environment* (2021).

[36] A. E. W. Adel, A. Aldurayhim, and A. El-Mesady, "Mathematical modeling and analysis of a novel monkeypox virus spread integrating imperfect vaccination and nonlinear incidence rates," *Ain Shams Engineering Journal*, vol. 15 (2024).

[37] D. Biswas and S. Pal, "Role of awareness to control transmission of hiv/aids epidemic with treatment and sensitivity analysis," *Journal of Statistics and Management Systems*, vol. 25, no. 3, pp. 617–644 (2022).

[38] D. Aldila, R. P. Dhanendra, S. H. Khoshnaw, J. W. Puspita, P. Z. Kamalia, and M. Shahzad, "Understanding hiv/aids dynamics: insights from cd4+ t cells, antiretroviral treatment, and countryspecific analysis," *Frontiers in Public Health*, vol. 12, p. 1324858 (2024).

[39] D. Aldila, B. D. H. A. Widyah, and G. Hartanti, "Strategies of optimal control for hiv spread prevention with health campaign," *Communications in Mathematical Biology and Neuroscience*, vol. 2020, no. 7 (2020).

[40] H. Nasir, "Population model of cardiovascular diseases: Global dynamics, sensitivity analysis, and optimal control," *Journal of Information and Optimization Sciences*, vol. 43, no. 4, pp. 781–800 (2022).

[41] M. A. Safi and A. B. Gumel, "Mathematical analysis of a disease transmission model with quarantine, isolation and an imperfect

vaccine," *Journal of Mathematical Analysis and Applications*, vol. 377, no. 1, pp. 317–339 (2011).

[42] H. Ben Fredj and F. Ch´erif, "Novel coronavirus disease infection in tunisia: Mathematical model and the impact of the quarantine strategy," *Chaos, Solitons Fractals,* vol. 138, p. 109913 (2020).

[43] Z. Yu, J. Zhang, Y. Zhang, X. Cong, X. Li, and A. M. Mostafa, "Mathematical modeling and simulation for covid-19 with mutant and quarantined strategy," *Journal of King Saud University - Science,* vol. 36, no. 1, p. 103791 (2024).

[44] Y. Gu, S. Ullah, M. A. Khan, M. Y. Alshahrani, M. Abohassan, and M. B. Riaz, "Mathematical modeling and stability analysis of the covid-19 with quarantine and isolation," *Results in Physics,* vol. 35, p. 106075 (2022).

[45] A. S. Alsheri, A. A. Alraeza, and M. R. Afia, "Mathematical modeling of the effect of quarantine rate on controlling the infection of covid-19 in the population of saudi arabia," *Materials Today: Proceedings,* vol. 62, pp. 3970–3975 (2022).

[46] P. Pandey, Y.-M. Chu, J. G´omez-Aguilar, H. Jahanshahi, and A. A. Aly, "A novel fractional mathematical model of covid-19 epidemic considering quarantine and latent time," *Alexandria Engineering Journal*, vol. 61, no. 5, pp. 4047–4059 (2022).

[47] A. Babaei, M. Ahmadi, H. Jafari, and A. Liya, "A mathematical model to examine the effect of quarantine on the spread of coronavirus," *Computational Methods for Differential Equations*, vol. 9, no. 1, pp. 26–38 (2021).

[48] A. Kouidere, L. EL Youssoufi, H. Ferjouchia, O. Balatif, and M. Rachik, "Optimal control of mathematical modeling of the spread of the covid-19 pandemic with highlighting the negative impact of quarantine on diabetics people with cost-effectiveness," *Mathematical Biosciences*, vol. 340, p. 108702 (2021).

[49] A. Srivastava and Nilam, "Optimal control of a fractional order seiqr epidemic model with nonmonotonic incidence and quarantine class," *Journal of King Saud University - Science,* vol. 36, no. 2, p. 102582 (2024).

[50] R. R. Musafir, A. Suryanto, I. Darti, and Trisilowati, "Stability analysis of a fractional-order monkeypox epidemic model with quarantine and hospitalization," *Results in Control and Optimization,* vol. 6, pp. 34–50 (2024).

[51] Hendratno, "Covid-19 indonesia," Dataset, 2020, accessed: 2024-06-17. [Online]. Available: https://www.kaggle.com/datasets/hendratno/covid19-indonesia

[52] O. Diekmann, J. Heesterbeek, and M. Roberts, "The construction of next-generation matrices for compartmental epidemic models," *Journal of the Royal Society Interface*, vol. 7, pp. 873–885 (2010).

[53] D. Aldila, N. Awdinda, Fatmawati, F. F. Herdicho, M. Z. Ndii, and C. W. Chukwu, "Optimal control of pneumonia transmission model with seasonal factor: Learning from jakarta incidence data," *Heliyon*, vol. 9, no. 7 (2023).

[54] D. Aldila, "Dynamical analysis on a malaria model with relapse preventive treatment and saturated fumigation," *Computational and Mathematical Methods in Medicine* (2022).

[55] D. Aldila, J. P. Cháavez, K. P. Wijaya, N. C. Ganegoda, G. M. Simorangkir, H. Tasman, and E. Soewono, "A tuberculosis epidemic model as a proxy for the assessment of the novel m72/as01e vaccine," Elsevier, vol. 120 (2023).

[56] B. Song, C. Castillo-Chavez, and J. P. Aparicio, "Tuberculosis models with fast and slow dynamics: The role of close and casual contacts," *Mathematical Biosciences*, vol. 180, no. 1-2, pp. 187–205 (2002).

Received October, 2024